Journal of Physics: Conference Series **190** (2009) 012141 doi:10.1088/1742-6596/190/1/012141

Structure of $[Ru(bpy)_n(AP)_{(6-2n)}]^{2+}$ homogeneous complexes: DFT calculation vs. EXAFS

Luca Salassa [1], Diego Gianolio[2], Claudio Garino[2], Giovanni Salassa[2], Elisa Borfecchia,[2] Tiziana Ruiu[2], Carlo Nervi[2], Roberto Gobetto[2], Ranieri Bizzarri[3], Peter J. Sadler[1], and Carlo Lamberti[2]

(1) Department of Chemistry, University of Warwick Gibbet Hill Road, Coventry (CV4 7AL), United Kingdom.

(2) Department of Inorganic, Materials and Physical Chemistry, NIS Centre of Excellence and INSTM unit, University of Turin, Via P. Giuria 7, I-10125 Turin, Italy.

(3) Laboratorio NEST, Scuola Normale Superiore di Pisa, Complesso San Silvestro, Piazza San Silvestro 12, 56127, Pisa, Italy.

L.Salassa@warwick.ac.uk

Abstract. We used EXAFS and DFT calculations to investigate the structure of $[Ru(bpy)(AP)_4]^{2+}$ and $[Ru(bpy)_2(AP)_2]^{2+}$ (bpy=2-2'-bipyridyne, AP=4-aminopyridyne) in aqueous solution (10 mM). These derivatives are of potential interest since, upon direct irradiation, they can form reactive aqua-species able to bind to macromolecules. An attempt has been made to determine with EXAFS the structure of the photodissociation product of the $[Ru(bpy)_2(AP)_2]^{2+}$ complex, where a water molecule fill the coordination vacancy left by an AP ligand resulting in $[Ru(bpy)_2(AP)(H_2O)]^{2+}$. Unfortunately, co-presence in the experimental sample of both original and photodissociated complexes, causes the failure of the analysis. This failure was due to the structural complexity of both systems and to the similarity in their EXAFS signals. This work underlines the potentialities and the limits of EXAFS spectroscopy when dealing with highly diluted samples where the local environment of the adsorbing atom is characterized by structured ligands: the local environment of Ru is correctly reproduced when dealing with homogeneous samples, while the co-presence of two or more different species makes the data analysis highly critical.

1. Introduction

Since the discovery of the antitumoural properties of cisplatin in 1965,[1] transition-metal-based compounds have been widely used in clinic as chemotherapeutic agents. Recently, it has been demonstrated that light can be used to activate anticancer metal complexes. Photochemical activation of an appropriate precursor provides a procedure for controlling the site, timing, and dosage of the metal complex, reducing undesired effects in other tissues or organs. Light-irradiation of metal complexes can induce, for example, the formation of very reactive species, as well as promoting selective interaction between metal complexes and target macromolecules (DNA, proteins).[2]

In our attempt to develop photoactive metal complexes and study their excited-state chemistry,[3] two Ru-derivatives of potential interest for chemotherapy and their photodissociated products were studied with EXAFS.[4] The experiment was performed at ESRF beamline BM29, acquiring data both in transmission and in fluorescence mode. In particular solutions of $[Ru(bpy)_2(AP)_2]^{2+}$ and $[Ru(bpy)(AP)_4]^{2+}$ in water before and after light exposure were investigated (bpy=2-2'-bipyridyne, AP=4-aminopyridyne). Although the transmitted spectra were characterized by an edge jump of only 0.03 and 0.05, the quality of the $\chi(k)$ function is impressive and in perfect agreement with corresponding function extracted from fluorescence data. The EXAFS results are compared with the structural data obtained by density functional theory (DFT) calculations.

2. Experimental and Methods

Details on the materials preparation are reported elsewhere.[4]

2.1. EXAFS data collection

X-ray absorption experiments, at the Ru K-edge (22117 eV), were performed at the BM29 of the ESRF facility (Grenoble, F). The white beam was monochromatized using a Si(111) double crystal; harmonic rejection was performed by detuning the crystals at 20% of the rocking curve. Energy calibration was at 23222 eV using a Rh metal foil. $[Ru(bpy)_3]Cl_2$ model compound was measured in transmission mode by uniformly diluting the sample in BN and preparing a self-supported pellet of optimized thickness. An EXAFS cell, specifically devoted to liquid samples, was filled with an aqueous solution of $[Ru(bpy)(AP)_4]Cl_2$ or $[Ru(bpy)_2(AP)_2]Cl_2$ just below the saturation limit (10 mM). Corresponding liquid complexes were thus measured in their cationic forms: $[Ru(bpy)(AP)_4]^{2+}$ and $[Ru(bpy)_2(AP)_2]^{2+}$. Due to Ru dilution, EXAFS spectra were collected in fluorescence mode, by means of a 13-element germanium monolithic detector, collecting the Ru $K_{\alpha 1\text{-}3}$ fluorescence lines in the 18500–19500 eV range. To limit the flux of elastically-scattered photons (21800–23500 eV), a Mo filter (acting as a low-band pass filter with threshold at 20000 eV) was inserted between the sample and the fluorescence detector. This insertion allowed the sample-to-detector distance to be minimized (thus maximizing the solid angle seen by the detector and consequently the Ru $K_{\alpha 1\text{-}3}$ fluorescence photons). The intensity of the incident beam was monitored by an ionization chamber. The beam transmitted through the sample passed further through a second ionization chamber, resulting in a transmission EXAFS spectrum characterized by edge jump of 0.03 and 0.05 in the two cases. The XANES part of the spectra was acquired with an energy step of 1 eV and an integration time of 2 s/point. The EXAFS part of the spectra was collected with a variable sampling step in energy, resulting in $\Delta k = 0.03$ Å^{-1}, up to 18 Å^{-1}, with an integration time that linearly increases with k from 2 to 20 s/point to account for the low signal-to-noise ratio at high k values. The extraction of the $\chi(k)$ function was performed using Athena programs.[5] For both samples, three consecutive EXAFS spectra were collected, resulting in three μx spectra (obtained by integrating the counts of the 13 elements of the detector), and corresponding $\chi(k)$ functions were averaged before data analysis.

2.2. Computational details

All ground-state geometry optimization calculations were performed with the Gaussian 03 code[6] employing the DFT method with Becke's three parameter hybrid functional[7] and Lee-Yang-Parr's gradient corrected correlation functional[8] (B3LYP). The LanL2DZ basis set[9] and effective core potential were used for the Ru atom and both the split-valence 6-31G** and 6-311G** basis sets[10] were applied for all other atoms. Geometry optimizations of both complexes were determined in water solution; the conductor-like polarizable continuum model method was employed to mimic solvent effects.[11] Figure 1 reports the so optimized structures.

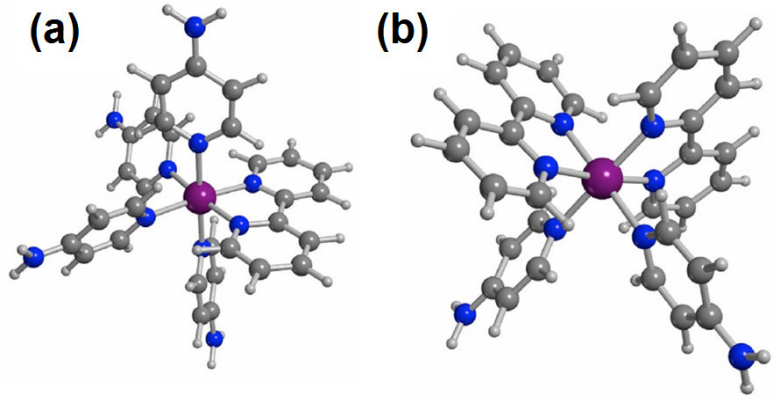

Figure 1: Ruthenium complexes $[Ru(bpy)(AP)_4]^{2+}$ and $[Ru(bpy)_2(AP)_2]^{2+}$ structures, obtained by optimization of DFT calculation part (a) and (b) respectively. The violet central atom is the Ru, the blue atoms represents the N and the grey ones are C.

3. Results and Discussion

3.1. EXAFS data analysis

For both samples, three consecutive EXAFS spectra were collected, resulting in three μx spectra (obtained by integrating the counts of the 13 elements of the detector), and corresponding χ(k) functions were averaged before data analysis. Analogously, the three EXAFS spectra, simultaneously collected in transmission mode, were extracted and corresponding χ(k) functions averaged before data analysis, resulting in the $k^2\chi(k)$ function reported in Figure 2.

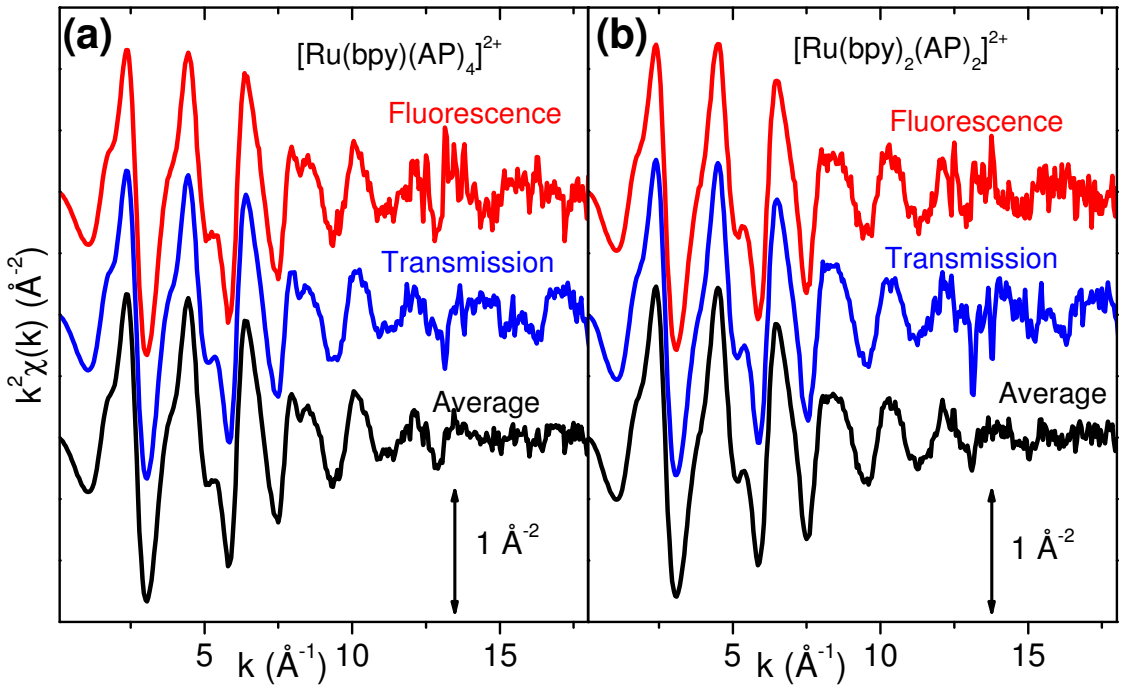

Figure 2. k^2-weighted χ(k) function obtained averaging along the three scans the fluorescence (red top curves) and the transmission (blue middle curves) EXAFS spectra. The bottom black curves report the $k^2\chi(k)$ function obtained averaging the fluorescence and the transmission χ(k) functions. Parts (a) and (b) refer to $[Ru(bpy)(AP)_4]^{2+}$ and $[Ru(bpy)_2(AP)_2]^{2+}$ complexes, respectively.

The quality of the $\chi(k)$ functions obtained from the transmitted spectra (blue curves in Figure 2) is impressive for samples with so low edge jumps, and is due to the high homogeneity of the liquid samples and on the high stability of BM29 beamline. For both samples, the EXAFS data analysis performed on the fluorescence and transmission data sets resulted, within experimental errors, in the same values for all optimized parameters (not reported for brevity). Consequently, the fluorescence and transmission data sets were averaged, resulting in the black spectra in Figure 2. The same data analysis was repeated for the final averaged data set, (vide infra Figure 3 and Table 1), resulting in optimized parameters compatible with those obtained in the two previous analyses, but characterized by smaller error bars. EXAFS data analysis was performed using the Arthemis software.[5] Phase and amplitude functions were calculated by FEFF6 code[12] using as input the structure obtained from DFT calculations (see Figure 1). Phase and amplitudes were successfully checked with $[Ru(bpy)_3]Cl_2$ as a model compound, measured in transmission mode with the same sampling procedure described for the liquid sample (only two spectra were collected in this case). For each sample the averaged $k^2\chi(k)$ function was Fourier transformed in the $\Delta k = 2.00–18.00$ Å^{-1} interval. The fits were performed in R-space in the $\Delta R = 1.00–5.00$ Å range ($2\Delta k\Delta R/\pi > 40$). Due to the complexity of the structure, more than 150 single scattering (SS) and multiple scattering (MS) paths contribute to the overall EXAFS signal. By excluding the paths having an amplitude smaller than 5% of the most intense one (the Ru–N SS path around 2.11 Å for the closest bpy unit), more than 70 paths were included in the fit. To limit the number of optimized variables, all paths were optimized with the same amplitude factor (S_0^2) and with the same energy shift parameter (ΔE). Moreover, both the AP and bpy ligands were considered as rigid molecules for which the only degree of freedom is a radial translation along the corresponding Ru–N axis. The different AP ligands are assumed to behave in the same way, and the same was inferred for the two bpy rings of the $[Ru(bpy)_2(AP)_2]^{2+}$ complex. As a consequence, the only two structural parameters optimized in the fit are $R_{Ru–N(AP)}$ and $R_{Ru–N(bpy)}$, being the lengths of all other paths computed from the $R_{Ru–N(AP)}$ and $R_{Ru–N(bpy)}$ values according to geometrical constraints imposed by the rigidity of the AP and bpy entities. Neglecting the inter-ligand vibrations of the AP and bpy units, only two Debye-Waller factors were optimized, $\sigma_{Ru–N(AP)}$ and $\sigma_{Ru–N(bpy)}$, for all the SS paths involving AP or bpy atoms, respectively. MS paths involving atoms of different AP (or of different bpy) units were simulated with a Debye-Waller factor of $\sigma_{MS} = 4\sigma_{Ru–N(AP)}$ (or of $4\sigma_{Ru–N(bpy)}$); MS paths involving atoms of a AP and of a bpy units were simulated with a Debye-Waller factor of $\sigma_{MS} = \sigma_{Ru–N(AP)} + \sigma_{Ru–N(bpy)} + 2\mathrm{sqrt}[\sigma_{Ru–N(AP)}\,\sigma_{Ru–N(bpy)}]$.

3.2. EXAFS results on the $[Ru(bpy)_3]Cl_2$ model compound

The quality of the fit obtained for the $[Ru(bpy)_3]Cl_2$ model compound can be observed in the top spectra of Figure 3. Looking to the optimized parameters (Table 1), we obtain a negligible energy shift, an S_0^2 equal to unit within the experimental incertitude, a Debye-Waller Factor of 0.0028 Å^2 and a Ru–N distance that is shorter by 0.05 Å with respect to the value obtained from DFT calculations. The quality of the fit can be further confirmed by the very low values of the associated errors and by the low correlations among the 4 fitted parameters: $S_0^2/\sigma = 0.75$ and $\Delta E/R_{Ru–N} = 0.71$, all other correlations are below 0.25 in absolute value.

3.3. EXAFS results for the $[Ru(bpy)(AP)_4]^{2+}$ and $[Ru(bpy)_2(AP)_2]^{2+}$ complexes

Once the EXAFS of the $[Ru(bpy)_3]Cl_2$ model compound was correctly reproduced, we proceeded on the analysis of the EXAFS spectra of $[Ru(bpy)(AP)_4]^{2+}$ and $[Ru(bpy)_2(AP)_2]^{2+}$ complexes as described in Section 3.1.

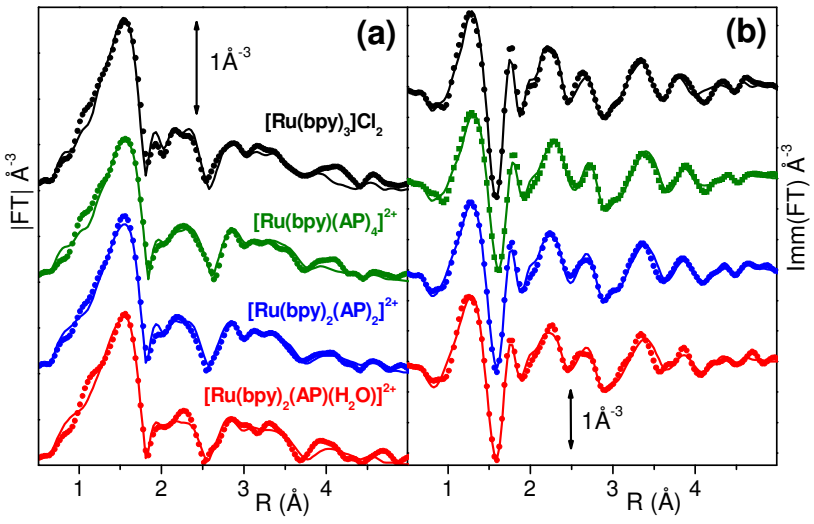

Figure 3. Comparison between experimental (scattered curves) and corresponding best fits (solid lines) for, from top to bottom: $[Ru(bpy)_3]Cl_2$, $[Ru(bpy)(AP)_4]^{2+}$, $[Ru(bpy)_2(AP)_2]^{2+}$ and $[Ru(bpy)_2(AP)(H_2O)]^{2+}$ complexes. Parts (a) and (b) report the modulus and the imaginary parts, respectively. For quantitative values of the parameters optimized in the fits, see Table 1.

Table 1. Summary of the parameters optimized in the fitting of the EXAFS data (Figure 2) on the $[Ru(bpy)_3]Cl_2$ model compound, on the $[Ru(bpy)(AP)_4]^{2+}$ and $[Ru(bpy)_2(AP)_2]^{2+}$ complexes and on the photodissociated product of the latter: $[Ru(bpy)_2(AP)(H_2O)]^{2+}$. The fits were performed in R-space in the 1.0–5.0 Å range over k^2-weighted FT of the $\chi(k)$ functions performed in the 2.0–18.0 Å^{-1} interval. A single ΔE_0 and a single S_0^2 were optimized for all SS and MS paths. Not optimized parameters are recognizable by the absence of corresponding error bars. Optimized bond distances are compared to the average values obtained from DFT calculations given in parenthesis.

complex	$[Ru(bpy)_3]Cl_2$	$[Ru(bpy)(AP)_4]^{2+}$	$[Ru(bpy)_2(AP)_2]^{2+}$	$[Ru(bpy)_2(AP)(H_2O)]^{2+}$
N_{ind}	40	40	40	40
N_{fit}	4	6	6	6
R_{factor}	0.039	0.031	0.032	0.050
S_0^2	1.05 ± 0.05	1.03 ± 0.06	1.00 ± 0.05	1
ΔE (eV)	-0.1 ± 0.4	-0.0 ± 0.4	-0.2 ± 0.4	0
$R_{N(bpy)}$ (Å)	2.056 ± 0.004 (2.106)	2.09 ± 0.01 (2.114)	2.069 ± 0.009 (2.114)	2.05 ± 0.01 (2.101)
$\sigma_{N(bpy)}$ (Å^2)	0.0028 ± 0.0004	0.003 ± 0.001	0.0029 ± 0.0007	0.0026 ± 0.0009
$R_{N(AP)}$ (Å)	-	2.09 ± 0.01 (2.188)	2.06 ± 0.03 (2.181)	2.10 ± 0.03 (2.166)
$\sigma_{N(AP)}$ (Å^2)	-	0.005 ± 0.001	0.006 ± 0.003	0.004 ± 0.003
R_{OH2} (Å)	-	-	-	2.06 ± 0.05 (2.256)
σ_{OH2} (Å^2)	-	-	-	0.009 ± 0.007

As for the model compound, for both aqua complexes we obtained ΔE and S_0^2 compatible with zero and unit, respectively. Because bpy units contribute almost twice than the AP ones to the high distance paths, corresponding distances and Debye-Waller factors are determined with a better precision. Within the experimental incertitude, that is very small in both cases, the Debye-Waller factor of bpy units is the same in $[Ru(bpy)_3]Cl_2$, $[Ru(bpy)(AP)_4]^{2+}$ and $[Ru(bpy)_2(AP)_2]^{2+}$ complexes (Table 1). Accordingly to the lower mass, the AP units of the aqua complexes exhibit a Debye-Waller factor that is almost twice that of the bpy ones. DFT calculations predict that, moving from $[Ru(bpy)_3]Cl_2$ to $[Ru(bpy)(AP)_4]^{2+}$ (or to $[Ru(bpy)_2(AP)_2]^{2+}$), the insertion of four (two) AP units, substituting two (one) bpy one, results in an increasing of the $R_{N(bpy)}$ distance by 0.008 Å. For the $[Ru(bpy)(AP)_4]^{2+}$ complex, the experimental result confirm a stretching of 0.034 ± 0.014 Å, for the $[Ru(bpy)_2(AP)_2]^{2+}$ complex the result is borderline with the incertitude (0.013 ± 0.013 Å). The nitrogen atom of the AP units is located at 2.09 ± 0.01 Å and at 2.06 ± 0.03 Å for the $[Ru(bpy)(AP)_4]^{2+}$

and $[Ru(bpy)_2(AP)_2]^{2+}$, respectively. Both values are shorter than the value predicted by the DFT calculations (Table 1). Curiously, the optimized $R_{N(bpy)}$ and $R_{N(AP)}$ distances become very close, to be considered as equivalent owing to the large error associated to $R_{N(AP)}$.[13] The higher correlation among parameters occurs for $R_{N(AP)}/R_{Ru-N(bpy)} = -0.82$ (−0.85), $\sigma_{N(AP)}/\sigma_{N(bpy)} = -0.62$, (−0.63), $S_0^2/\sigma_{N(AP)} = 0.64$ (0.62), and $\Delta E/R_{N(AP)} = 0.57$ (0.56) for $Ru(bpy)(AP)_4]^{2+}$ ($[Ru(bpy)_2(AP)_2]^{2+}$) complex. All other correlations are below 0.25 in absolute value. Summarizing, we conclude that the EXAFS data analysis fully confirms the overall structure optimized by DFT calculations, being the experimental Ru−N distances systematically shorter by some hundredths of Å.

3.4. EXAFS results on the photodissociated $Ru(bpy)_2(AP)(H_2O)]^{2+}$ complex.

From NMR in aqueous solution we know that the photo-dissociation process is not complete and the sample exposed to prolonged irradiation still contains a fraction of $[Ru(bpy)_2(AP)_2]^{2+}$ together with its photodissociated product $[Ru(bpy)_2(AP)(H_2O)]^{2+}$. Therefore, the fit reported in the last column of Table 1 is intrinsically incorrect. The structural model of the photodissociated system differs from the original $[Ru(bpy)_2(AP)_2]^{2+}$ one by the loss of a AP ring, substituted by a water molecule. As the scattering power of the O atom of the additional H_2O molecule is virtually indistinguishable from the N atom one of the lost AP, the main difference between $[Ru(bpy)_2(AP)_2]^{2+}$ and its photodissociated homologue lies in the absence of all SS and MS paths related to the dislodged AP ring. This implies the addition of two parameters in the fit for the Ru−OH_2 distance and for its corresponding Debye-Waller factor. The addition of a further independent contribution in the same R-range of the Ru−N SS paths of both AP and bpy units results in a fit instability giving rise to excellent mathematical agreement with the experimental data but with non-physical outputs for distances and Debye-Waller factors. In order to, at least partially, overcome this problem (at least partially), we have fixed S_0^2 and ΔE to 1 and 0 eV, respectively. The decrease of the parameter $\sigma_{N(AP)}$, from 0.006 to 0.004 $Å^2$, is thus a consequence of the fact that, in average, each Ru atoms has more than one AP ligand, confirming that a fraction of undissociated molecules is still present. The optimized R_{OH2} distance at the same value that of the Ru−N distances (shorter by 0.2 Å from the DFT value) is a further proof of this statement. We consequently decided to try a two phase fit.[14] A phase fraction parameter x was added to the fit, weighting the signals of the undissociated molecule and of the photodissociated one by $(1-x)$ and x, respectively. In order to keep limited the number of optimized parameters, for both phases, the parameters S_0^2 and ΔE were fixed to 1 and 0 eV, the distances and Debye-Waller factors of both AP and bpy rings were fixed to the output of the fit obtained from the pure $[Ru(bpy)_2(AP)_2]^{2+}$ complex. This fit, having only three free parameters, gave the following results: $x = 0.30 \pm 0.13$; $R_{OH2} = 2.49 \pm 0.07$ Å and $\sigma_{OH2} = 0.002 \pm 0.007$ $Å^2$, resulting in $R_{factor} = 0.047$. The extremely high values of the associated error parameters, as well as the unexpected optimized values, imposes to check the validity of these outputs.[15] We decided to perform eleven fits optimizing only R_{OH2} and σ_{OH2} by fixing x from 0 to 1 by steps of 0.1. The results of these fits are reported in Figure 4. Part (a) reports the optimized σ_{OH2} vs. x, the two horizontal lines define the interval of physical acceptance of the parameter. Figure 4b shows that the optimized R_{OH2} progressively decreases upon increasing x up to $x = 0.45$; for higher photodissociated fraction, its value remains very close to the Ru−N distance, clearly evidencing the lack of N ligand for too high x values.

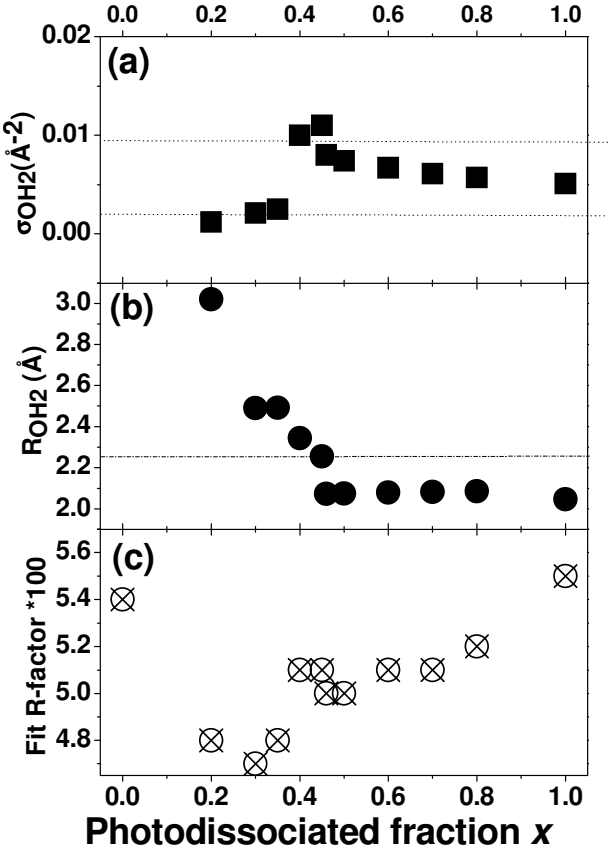

Figure 4. Evolution of the water Debye-Waller factor (part a), of the Ru–OH_2 bond distance (part b) and of the R-factor of the fit (part c) in a series of 2-phases fits imposing the fraction *x* of the photodissociated product $[Ru(bpy)_2(AP)(H_2O)]^{2+}$.

The evolution of the R factor of the fits vs. *x* (Figure 4c), confirms the value of: $x = 0.30$ obtained in the fit performed leaving *x* free, but the shape around the minimum is far to be regular.

4. Conclusions

Ru K-edge EXAFS data analysis on $[Ru(bpy)(AP)_4]^{2+}$ and $[Ru(bpy)_2(AP)_2]^{2+}$ in aqueous solution validates the structure optimized by DFT calculations. Just a small contraction of both $R_{N(bpy)}$ and $R_{N(AP)}$ distances of few hundredths of Å is observed from experiment. For both complexes the Debye-Waller factor of the bpy ligand is comparable to that optimized in the $[Ru(bpy)_3]Cl_2$, while the AP ligand one scales according to what's expected from the ligands masses ratio. Notwithstanding the sample dilution (10 mM), the high homogeneity of both solutions allowed us to refine the complex structure of both systems with high accuracy up to 5 Å around Ru.

The interest of such complexes lies in their ability to lost a ligand upon irradiation, resulting in reactive aqua-species able to bind to macromolecules. We consequently made an attempt to determine with EXAFS the structure of the photodissociation product of the $[Ru(bpy)_2(AP)_2]^{2+}$ complex, where a water molecule fill the coordination vacancy left by an AP ligand resulting in $[Ru(bpy)_2(AP)(H_2O)]^{2+}$. Unfortunately, co-presence in the experimental sample of both original and photodissociated complexes, causes the failure of the analysis. In fact the fit of a single data set with two similar models implies a too high correlation among optimized parameters, making the fit output questionable.

Acknowledgements

We are indebted to C. Prestipino for his friendly and highly competent support during EXAFS data collection at BM29 beamline of the ESRF (Proposal CH-2604).

References

[1] B. Rosenberg, L. VanCamp and T. Krigas, *Nature*, 1965, **205**, 698.
[2] W.H. Ang, P.J. Dyson, *Eur. J. Inorg. Chem*., 2006, 4003.
F. S. Mackay, J. A. Woods, P. Heringova, J. Kasparkova, A. M. Pizarro, S. A. Moggach, S. Parsons, V. Brabec and P. J. Sadler, *Proc. Natl. Acad. Sci. U. S. A.,* 2007, **104**, 20743.
[3] C. Garino, T. Ruiu, L. Salassa, A. Albertino, G. Volpi, C. Nervi, R. Gobetto, K. I. Hardcastle, *Eur. J. Inorg. Chem*., 2008, 3587.
L. Salassa, C. Garino, A. Albertino, G. Volpi, C. Nervi, R. Gobetto, K. I.Hardcastle, *Organometallics*, 2008, **27**, 1427.
L. Salassa, C. Garino, G. Salassa, R. Gobetto, C. Nervi, *J. Am. Chem. Soc*., 2008, **130**, 9590.
C. Garino, R. Gobetto, C. Nervi, L. Salassa, E. Rosenberg, J. B. A. Ross, X. Chu, K. I. Hardcastle, C. Sabatini, *Inorg. Chem*., 2007, **46**, 8752.
A. Albertino, C. Nervi, C. Garino, S. Ghiani, R. Gobetto, L. Salassa, M. Milanesio, G. Croce, E. Rosenberg, A. Sharmin, R. Buscaino, G.Viscardi, *J. Organomet. Chem*., 2007, **692**, 1377.
F. S. Mackay, N. J. Farrer, L. Salassa, H-C. Tai, R. J. Deeth, S. A. Moggach, P. A. Wood, S. Parsons, P. J. Sadler, *Dalton Trans*., 2009, 2315.
[4] L. Salassa, C. Garino, G. Salassa, C. Nervi, R. Gobetto, C. Lamberti, D. Gianolio, R. Bizzarri and P. J. Sadler, *Inorg. Chem*., 2009, **48**, 1469.
[5] B. Ravel and M. Newville, *J. Synchrot. Radiat*., 2005, **12**, 537.
[6] M. J. Frisch, et al. Gaussian 03 2004.
[7] A. D. Becke, *J. Chem. Phys*., 1993, **98**, 5648.
[8] C. Lee, W. Yang, R. G. Parr, *Phys. Rev. B*, 1988, **37**, 785.
[9] P. J. Hay, R. W. Willard, *J. Chem. Phys.*, 1985, **82**, 270.
[10] A. D. McLean, G. S. Chandler, *J. Chem. Phys.* 1980, **72**, 5639.
R. Krishnan, J. S. Binkley, R. Seeger, J. A. Pople, *J. Chem. Phys*., 1980, **72**, 650.
[11] M. Cossi, N. Rega, G. Scalmani, V. Barone, *J. Comput. Chem*., 2003, 24, 669.
M. Cossi, V. Barone, *J. Chem. Phys*. 2001, **115**, 4708.
V. Barone, M. Cossi, *J. Phys. Chem. A,* 1998, **102**, 1995.
[12] A. L. Ankudinov, B. Ravel, J. J. Rehr and S. D. Conradson, *Phys. Rev. B*, 1998, **58**, 7565.
[13] This behavior is seems to be typical of the EXAFS technique. When several neighbors of the same chemical nature are located at close distances, there is a tendency to let the such distances to converge to a common value, see F. Bonino, S. Chavan, J. G. Vitillo, E. Groppo, G. Agostini, C. Lamberti, P. D. C. Dietzel, C. Prestipino, S. Bordiga, *Chem. Mater.,* 2008, **20**, 4957.
[14] C. Prestipino, S. Bordiga, C. Lamberti, S. Vidotto, M. Garilli, B. Cremaschi, A. Marsella, G. Leofanti, P. Fisicaro, G. Spoto and A. Zecchina, *J. Phys. Chem. B*, 2003, **107**, 5022.
E. Groppo, C. Prestipino, F. Cesano, F. Bonino, S. Bordiga, C. Lamberti, P. C. Thüne, J. W. Niemantsverdriet and A. Zecchina, *J. Catal*., 2005, **230**, 98.
J. Estephane, E. Groppo, A. Damin, J. G. Vitillo, D. Gianolio, C. Lamberti, S. Bordiga, C. Prestipino, S. Nikitenko, E. A. Quadrelli, M. Taoufik, J. M. Basset and A. Zecchina, *J. Phys. Chem. C*, 2009, **113**, 7305.
[15] R_{OH2} is 0.23 Å longer than the values optimized in the ab initio calculations and 0.43 Å longer than the value optimized fitting the EXAFS data with the pure photo-dissociated phase (see Table 1). Analogously σ_{OH2} is 4.5 times smaller than the value optimized fitting the EXAFS data with the pure photo-dissociated phase.